ORIGINAL RESEARCH

A Proposed Ordinal Scale for Grading Histology in Elastase-Induced, Saccular Aneurysms

D. Dai
Y.H. Ding
D.A. Lewis
D.F. Kallmes

BACKGROUND AND PURPOSE: The elastase-induced aneurysm model in rabbits, though widely applied, still offers no quantitative or qualitative metric for histologic outcome. This study is aimed at producing such a scale to evaluate outcome and facilitate meaningful, preclinical comparison among devices proposed for aneurysm treatment.

MATERIAL AND METHOD: Elastase-induced aneurysms were created and embolized in 30 rabbits. Aneurysms were harvested between 2 and 24 weeks. Specimens were embedded in paraffin, sectioned, and stained with hematoxylin and eosin. The scale comprised 3 subcategories: extent and degree of recanalization/coil compaction; neck healing, based on thickness and type of tissue across the neck; and dome healing. Neck healing was assessed by both gross and microscopic inspections. Compaction was assessed by using both the angiographic and histologic images. Dome healing was assessed by using the microscopic images only. Data were analyzed with either analysis of variance for the quantitative data or Kruskal-Wallis tests when analyzing the nonparametric data.

RESULTS: We noted a significant main effect for healing over time ($P = .0016$). Post hoc tests showed that, at 2 weeks, the mean score was 1.4 ± 0.8, as compared with a mean score of 7.2 ± 1.6 for the 24-week time point ($P \leq .05$). Further, significant differences in healing between narrow-necked (6.0 ± 1.3) and wide-necked aneurysms (3.5 ± 1.1) were seen at 4 weeks ($P = .0433$). The dynamic range of the scale also appears to be appropriate, because there was adequate range at the upper portion of the scale to reflect improved healing that might be achieved with future devices.

CONCLUSIONS: This scale is a potentially relevant outcome measurement tool for elastase-induced aneurysms after endovascular therapy. Future studies are still required to confirm its practical relevance.

Development of endovascular occlusion devices has been facilitated by the use of various animal models of saccular aneurysms. Detachable, platinum coils have been tested by using surgically created aneurysms in swine, canines, rabbits, and primates.[1-7] More recently, elastase-induced aneurysms in rabbits have been proposed as a useful preclinical tool for device development.[8-14]

Even though preclinical models have facilitated coil development, significant limitations in the preclinical evaluation of these devices remain. Specifically, quantification strategies for evaluating outcome—angiographic or histologic—have not been standardized within or between various animal models. Other investigators have proposed extent of neck coverage with thick membranes, neck tissue thickness, and angiographic recanalization as outcomes after embolization in sidewall aneurysms created in swine and canine models.[15-17] These assessment tools have largely been confined to single centers and have not been studied to confirm whether they can be generalized to other centers or to models in other species.

The elastase-induced aneurysm model in rabbits, though widely applied, still offers no quantitative or semiquantitative metric for outcome. The availability of an accurate, reproducible, and clinically relevant outcome measure after treatment of the elastase aneurysm model would speed preclinical development of new occlusion devices. Use of angiographic recanalization as an outcome in this model likely would be impractical, because angiographically apparent recanalization, even with standard coils, is uncommon in elastase-induced saccular aneurysms. We propose that a relevant assessment tool for aneurysm healing after coiling would be based on histology.

In this study, an ordinal scale for grading the degree of healing in the rabbit model of elastase-induced aneurysms has been developed and is proposed for use. The scale encompasses both gross and microscopic histologic findings. Experience with this model indicates that some features related to the extent of healing are best evaluated on the gross specimen, while details of the type of tissue are best evaluated with the microscopic histologic findings. Three subcategories—including extent and degree of recanalization/coil compaction, degree of neck healing, and type of tissue found within the aneurysm dome—could be considered relevant markers of outcome and thus comprise the scale.

We report our findings in a cohort of experimental aneurysms treated with standard platinum coils by using the new assessment tool and offer these normative data that may be used in future trials. In addition, because healing in humans is strongly correlated to aneurysm size, this study examined the range of total scores across time points and as a function of aneurysm neck size.

Methods

Aneurysm Creation Technique

Elastase-induced, saccular aneurysms were created in 30 New Zealand white rabbits (body weight 3–4 kg) by using the rabbit elastase model. All procedures were approved by our institution's animal care and use committee. Detailed procedures for aneurysm creation have been described elsewhere.[9] In brief, anesthesia was induced with an intramuscular injection of ketamine, xylazine, and acepromazine (75, 5, and 1 mg/kg, respectively). Using sterile technique, we exposed and ligated distally the right common carotid artery (RCCA). A 1–2-mm bev-

Received March 28, 2005; accepted after revision June 14.

From the Neuroradiology Research Laboratory, Department of Radiology, Mayo Clinic and Foundation, Rochester, Minn.

This work funded by National Institutes of Health grant NS42646.

Address correspondence to David F. Kallmes, MD, Mayo Clinic and Foundation, 200 First Street, SW, Rochester, MN 55905.

Table 1: Grading scale for elastase-induced saccular aneurysms

Scale Number	Grading Components			
	Gross Neck	Micro Neck	Neck Compaction	Dome
0	No coverage	Unorganized clot	Macro-concave	Blood clot (all)
1	<50% coverage	Fibrin	Micro-concave	Organized tissue in <1/3 of dome area
2	50–75% coverage	Fibrin with organized tissue	Flat	Organized tissue in 1/3–2/3 dome area
3	>75% coverage	Completely organized tissue, thickness ≤1/3 coil diameter	Convex	Organized tissue in >2/3 of dome area
4	N/A	Completely organized tissue, thickness >1/3 of coil diameter	N/A	Completely organized loose tissue
5	N/A	N/A	N/A	Completely organized dense fibrous or cellular tissue

eled arteriotomy was made, and a 5F vascular sheath (Cordis Endovascular, Miami Lakes, Fla) was advanced retrograde in the RCCA to a point approximately 3 cm cephalic to the origin of RCCA. A roadmap image (Advantx; General Electric; Milwaukee, Wisc) was obtained by injection of contrast through the sheath placed in a retrograde position in the RCCA. This permitted the operator to identify the junction between the RCCA and the subclavian and brachiocephalic arteries. A 3F Fogarty balloon (Baxter Healthcare, Irvine, Calif) was advanced, with fluoroscopic guidance through the sheath to the level of the RCCA origin and was inflated with iodinated contrast material (Omnipaque 300; Amersham Health, Princeton, NJ). Porcine elastase (approximately 200 U/mL; Worthington Biochemical, Lakewood, NJ) was incubated within the lumen of the common carotid above the inflated balloon for 20 minutes, after which the catheter, the balloon, and the sheath were removed. The RCCA was ligated below the sheath entry site, and the incision was sutured closed.

Coil Embolization Procedure

Aneurysms were permitted to mature for at least 21 days following creation before embolization was performed. The same anesthesia described in aneurysm creation was employed for this procedure. The right common femoral artery (RCFA) was surgically exposed by using sterile technique. The artery was ligated distally by using 4–0 silk suture, and a 22-gauge angiocatheter was advanced retrograde into the artery, followed by placement of a 5F vascular sheath. Heparin (100 U/kg) was administered intravenously through the sheath. A 5F catheter (Envoy; Cordis Neurovascular Systems, Miami Lakes, Fla) was advanced into the brachiocephalic artery. Using a coaxial technique, with continuous heparinized flush, we advanced an Excel (Target Therapeutics, Freemont, Calif) 2-marker microcatheter into the aneurysm cavity. The size of the aneurysm cavity was assessed by using direct comparison to radiopaque sizing devices during digital subtraction angiography (DSA). Aneurysms were embolized with platinum coils as described elsewhere.[8] Aneurysm cavities were densely packed in all cases. Following the embolization, a final control DSA was performed. The catheters and sheath were removed, the femoral artery ligated, and the incision closed.

Harvesting Procedure

At the time of sacrifice, the subjects were anesthetized as described in the previous procedures and then euthanized with a lethal injection of pentobarbital. The chest cavity was opened, and the mediastinum was dissected. The proximal great vessels, including the coil-embolized segment of aneurysm, were exposed and dissected free from surrounding tissues. Aneurysms were harvested at 2 weeks ($n = 5$), 4 weeks ($n = 8$), 10 weeks ($n = 5$), 12 weeks ($n = 6$), and 24 weeks ($n = 6$). Specimens were removed and were immediately fixed in 10% neutral buffered formalin for at least 24 hours, after which each aneurysm's neck orifice was exposed to evaluate the tissue coverage at the neck.

Histologic Processing

The fixed tissues were dehydrated in an ascending series of ethanol, cleared in xylene, and embedded in paraffin. By using an Isomet Low Speed Saw (Buehler, Lake Bluff, Ill) with a Series 15HC Diamond Blade and Isocut Fluid, the aneurysms were sectioned at 1000-μm intervals through the portion bearing metallic coils in a coronal orientation, allowing long-axis sectioning of the aneurysm neck. Under a dissecting microscope, the metallic coil fragments were carefully removed by using sharp-tipped forceps. Following removal of all coil fragments, the sections were re-embedded in paraffin blocks. These blocks were sectioned employing a microtome (Leica, Model RM2165; Leica Microsystems, Nussloch, Germany) with disposable blades at 5–6-μm intervals. Sections were then floated on a water bath at 42°C to remove the wrinkles, mounted on Superfrost Plus slides (Fisher Scientific, Pittsburgh, Penn), and permitted to dry overnight in oven at 37°C. At least 2 sections from each block were stained with hematoxylin (Richard-Allan Scientific, Kalamazoo, Mich) and Eosin (Surgipath) (H&E, Richmond, Ill) staining for histopathologic evaluation.

Histologic Grading System

The proposed system was developed to incorporate healing aspects along the neck and in the dome, with the neck response given slightly greater weight than the dome. The details of the grading system are provided in Table 1. The measures were selected based on prior experience with the model. Neck healing was assessed by both gross and microscopic inspection with potential scores for each ranging from 0 to 4. It was previously noted that healing at the neck tended to progress from unorganized thrombus to fibrin to thin layers of hypocellular tissue (Fig 1). If different areas of the aneurysm neck showed different levels of healing, intermediate scores (ie, 0.5) were employed. Scores from both gross and microscopic evaluations were averaged to yield a single neck score. Dome healing also tended to progress from unorganized thrombus but then progressed to loose granulation tissue and to loose meshlike tissue with a thin, amorphous extracellular matrix (Fig 2). Dome healing (range, 0–5) was assessed by using the microscopic images only. Compaction (range, 0–3) was assessed by using both the angiographic and histologic images (Fig 3). Recanalization/coil compaction at aneurysm neck was histologically defined as a concave interface with the parent artery.

Aneurysm Neck Grading

Because clinical studies have shown a strong, inverse relationship between persistent aneurysm occlusion and neck width, the diameter of the aneurysm neck size was assessed to correlate healing with neck width. Exact neck diameter can be difficult to quantify, so an ordinal scale to rank neck width was employed. A 5-point graded scale as an assessment of neck diameter was employed by using the contralateral CCA as a direct, internal control for comparison: grade 1, neck definitely more narrow than diameter of contralateral CCA; grade 2, probably more narrow; grade 3, equal diameter; grade 4, probably wider; and grade 5, neck definitely wider than contralateral CCA. The necks of aneurysms were characterized as 2 groups based on the neck score, including small- (scores ≤ 3) or broad-necked (scores >3).

Statistical Analysis

Data were analyzed for main effects with either analysis of variance for the quantitative data or Kruskal-Wallis tests (JMP; SAS Institute, Cary, NC) when analyzing the nonparametric data. When main effects were found to be significant, differences between pairs of means were elucidated with a Tukey Kramer HSD post hoc test.

Results

Aneurysm Size

Aneurysm sizes were measured on the basis of the DSA images, and the results are shown in Table 2. There were no significant differences between time points for aneurysm neck length, width, or height ($P > .05$).

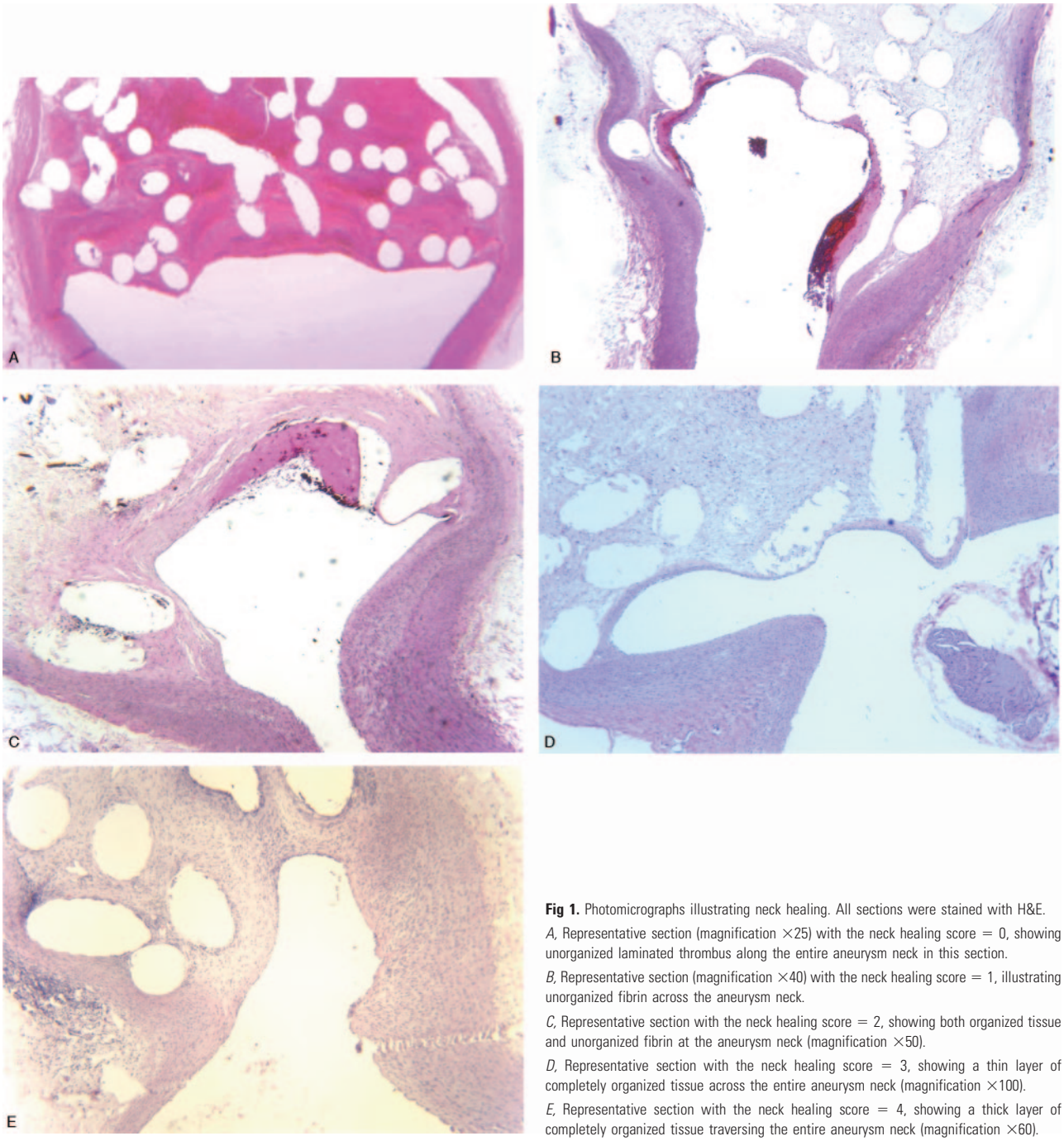

Fig 1. Photomicrographs illustrating neck healing. All sections were stained with H&E.

A, Representative section (magnification ×25) with the neck healing score = 0, showing unorganized laminated thrombus along the entire aneurysm neck in this section.

B, Representative section (magnification ×40) with the neck healing score = 1, illustrating unorganized fibrin across the aneurysm neck.

C, Representative section with the neck healing score = 2, showing both organized tissue and unorganized fibrin at the aneurysm neck (magnification ×50).

D, Representative section with the neck healing score = 3, showing a thin layer of completely organized tissue across the entire aneurysm neck (magnification ×100).

E, Representative section with the neck healing score = 4, showing a thick layer of completely organized tissue traversing the entire aneurysm neck (magnification ×60).

Histologic Scoring

The scoring data for each time point are shown in Fig 4. Histologic scores ranged from 0.5 to 8.8. A Kruskal-Wallis test revealed that there was a significant difference (= 0.0016) between time points for the ordinal, total score variables. Total scores increased significantly ($P \leq .05$) from a mean of 1.4 ± 0.8 at 2 weeks following implantation to a mean of 7.2 ± 1.6 at 24 weeks following implantation. A relative rapid and statistically significant increase in total score was noted between 2 weeks and 4 weeks (4.7 ± 1.8) after implantation ($P < .05$).

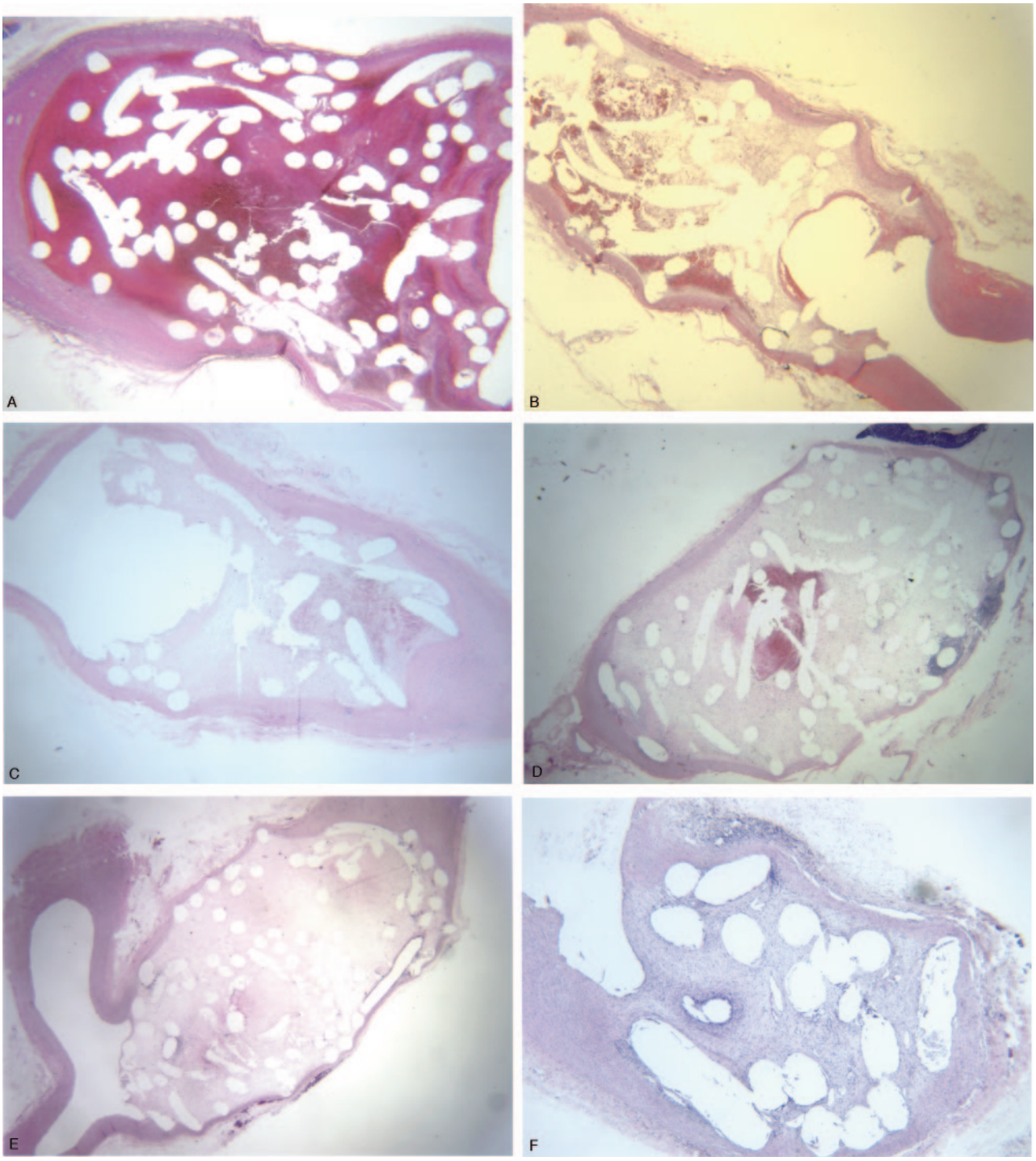

Fig 2. Photomicrographs illustrating dome healing. All sections were stained with H&E.

A, Representative section (magnification ×20) of a dome score = 0, showing that the aneurysm cavity is completely filled with unorganized thrombus.

B, Representative section (magnification ×15) when the dome score = 1, where less than one third of aneurysm cavity is filled with organized tissue.

C, Representative section (magnification ×20) with dome score = 2, in that approximately one half of the aneurysm cavity is filled with organized tissue.

D, Representative section (magnification ×15) with a dome score = 3, most the aneurysm cavity filled with organized tissue; a residual small area of unorganized thrombus is also evident.

E, Representative section (magnification ×15) with the dome score = 4, showing the aneurysm cavity to be entirely filled with loose organized tissue.

F, Representative section (magnification ×40) with the dome score = 5. Staining in this section reveals the aneurysm cavity is completely filled with attenuated cellular tissue.

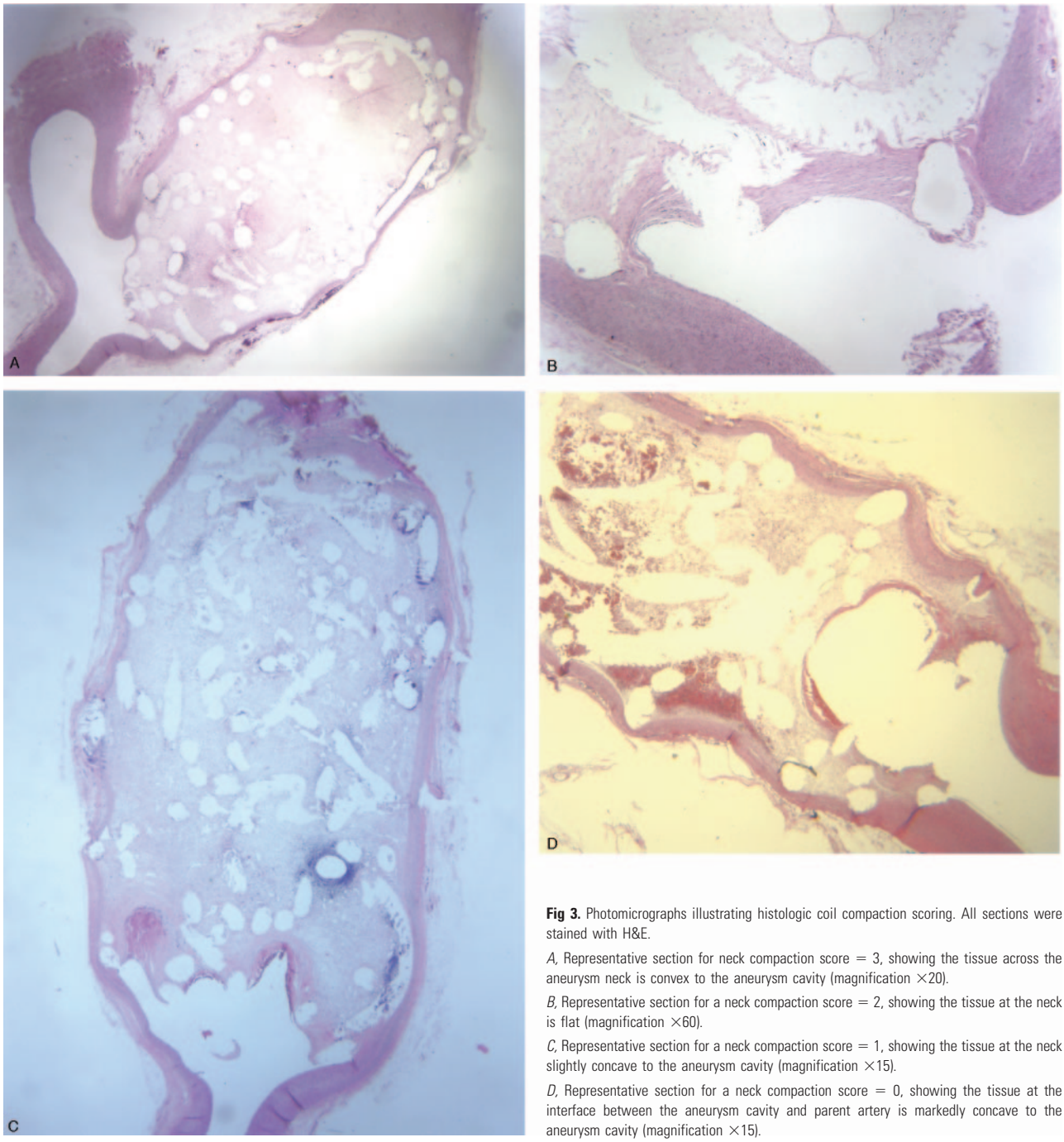

Fig 3. Photomicrographs illustrating histologic coil compaction scoring. All sections were stained with H&E.

A, Representative section for neck compaction score = 3, showing the tissue across the aneurysm neck is convex to the aneurysm cavity (magnification ×20).

B, Representative section for a neck compaction score = 2, showing the tissue at the neck is flat (magnification ×60).

C, Representative section for a neck compaction score = 1, showing the tissue at the neck slightly concave to the aneurysm cavity (magnification ×15).

D, Representative section for a neck compaction score = 0, showing the tissue at the interface between the aneurysm cavity and parent artery is markedly concave to the aneurysm cavity (magnification ×15).

Beyond 4 weeks, only mild increases in score were noted that did not differ significantly ($P > .05$; Table 3).

There were no differences in total score between small- and broad-necked aneurysms at 2 weeks. In contrast, the 4-week broad-necked aneurysms (1.5 ± 0.4) had significantly less healing in the dome ($P = .0172$) than the small-necked aneurysms (3.3 ± 0.5). The dominant histologic appearance of the aneurysm dome in chronic samples was that of a hypocellular, loose, meshlike tissue, with thin, faintly stained amorphous material and thin-walled vessels. This dome difference reinforced a significantly ($P = .0433$) smaller total score for the broad-necked group (3.5 ± 1.1) compared with the small-necked aneurysms (6.0 ± 1.3) at 4 weeks (Fig 5). There were no differences in neck scores, dome scores, compaction, and total scores at the more chronic time points.

Discussion

In this study, an ordinal measure of healing after experimental aneurysm embolization in rabbits is described. At the 2-week time point, the mean healing score was 1.4 ± 0.8, as compared with a mean healing score of 7.2 ± 1.6 for the later 24-week time point. These data indicate that the scale is capable of detecting differences in healing across time. Further, the dynamic range of the scale seems appropriate, because there is adequate range at the upper portion of the scale to reflect improved healing that might be achieved with new, modified

Table 2: Summary of aneurysm sizes by time

Duration (weeks)	Neck (mm)	Width (mm)	Height (mm)
2	3.1 ± 1.2	4.2 ± 0.8	9.8 ± 1.3
4	3.4 ± 1.0	4.4 ± 0.7	9.2 ± 1.8
10	4.0 ± 1.3	4.9 ± 1.1	9.1 ± 1.0
16	3.2 ± 0.9	4.0 ± 1.3	8.2 ± 1.9
24	3.2 ± 0.7	3.8 ± 0.8	8.4 ± 2.0

Note:—Data are represented as the mean ± SD. There were no significant differences between time points.

Table 3: Summary of histologic scores

	Gross Neck	Micro Neck	Compaction	Dome	Total Score
2 wk (n = 5)	0.0 ± 0.0	0.2 ± 0.3	0.8 ± 0.8	0.5 ± 0.4	1.4 ± 0.8
4 wk (n = 7)	1.3 ± 1.3	1.7 ± 1.0	0.9 ± 0.7	2.4 ± 1.0*	4.7 ± 1.8*
10 wk (n = 5)	0.8 ± 1.3	0.9 ± 1.2	0.4 ± 0.5	2.8 ± 1.4*	4.1 ± 2.5
16 wk (n = 4)	1.5 ± 0.6	2.1 ± 0.9*	1.1 ± 0.7	3.8 ± 0.4*†	6.5 ± 1.0*
24 wk (n = 6)	1.7 ± 1.2	2.4 ± 1.0*	1.2 ± 0.8	4.0 ± 0.0*†	7.2 ± 1.6*£

Note:—Data are represented as the mean ± SD.
* Variable is significantly different from the 2-week mean.
† Variable is significantly different from the 4-week mean.
£ Variable is significantly different from the 10-week mean.

devices. Specifically, the maximum score that can be achieved in this scale is 11.5 and the highest value in this study was 8.8. This proposed scale could potentially be a relevant measurement tool for elastase-induced aneurysms after endovascular therapy. Further studies by other investigators by using this tool are still required to confirm its practical relevance.

There was a small decrease in total score at 10 weeks, which was not statistically significant. This decrease could be attributed to the relatively large size/volume of the aneurysms treated at this time point as well as the small sample size ($n = 5$).

Early data are offered regarding the effect of aneurysm neck size on outcome employing this ordinal scale. These data suggest a difference in healing as a function of neck size, as seen clinically, but further studies will be required to better define this effect. It is important to note that the impact of aneurysm neck size (small- versus broad-necked) was seen only at 4 weeks following embolization and suggests that future preclinical studies might best be focused on broad-necked aneurysms at or around 4 weeks following implantation.

This assessment tool focused on 3 separate subcategories of healing, 2 that reflect healing at the neck and one that reflects healing in the dome. The ideal mechanism of healing along the aneurysm neck would be reconstitution of the normal vessel wall, including an endothelium, intima, and media. Such perfect reconstitution of a normal vessel wall, complete with internal and external elastic lamellae within highly organized medial smooth muscle layers, is unlikely to occur along any vascular implant; however, a well-developed neointima, with disorganized layers of myofibroblasts, might be considered a successful response. This scale was designed in light of this idealized and expected histologic response to a bioactive implant. Specifically, findings of unorganized thrombus or thin layers of fibrin were assigned low scores, as were gross findings of absent tissue coverage. Conversely, thick layers of tissue along the neck comprising spindle cells, which suggests neointimal formation, along with thick membranes observed grossly were given high scores in our scale.

Two metrics of neck healing, both gross and microscopic, were employed to reflect inherent limitations in either observation alone. Gross coverage may be difficult to quantify, in light of the relatively small size of the aneurysm neck. Microscopic neck coverage may be an artifact altered by sampling error, because only a few representative cross-sections will be seen for any single case. To address these limitations, both gross and microscopic findings of healing are cataloged; then the 2 scores were averaged into a single neck score.

In addition to the neck, the scale was structured to reflect idealized healing within the aneurysm dome. Unorganized or poorly organized thrombus offered poor mechanical integrity, whereas the presence of highly organized densely infiltrated smooth muscle-like cells offered excellent structural integrity. This tool reflects those considerations.

Previous authors have used both angiographic and histologic outcomes to assess healing in preclinical models. Raymond et al used angiographic evidence of recanalization in a canine aneurysm model.[17] Unfortunately, in the rabbit elastase model angiographically evident recanalization is uncom-

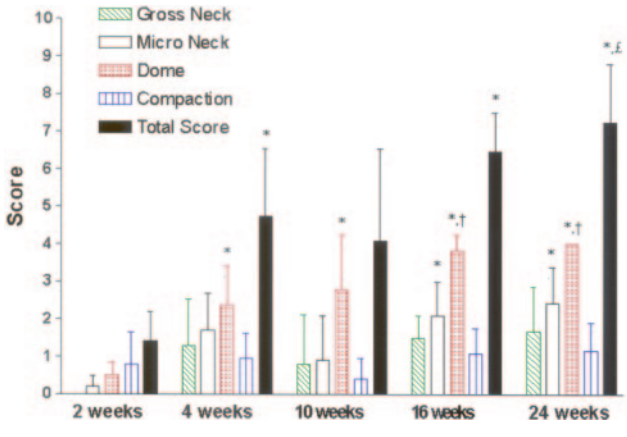

Fig 4. Mean and SD for scoring categories, in addition to Total Score, over survival time in weeks. Different colored bars represent the mean ± SD for each variable in the ordinal scale at 2 weeks (n = 5), 4 weeks (n = 8), 10 weeks (n = 5), 16 weeks (n = 6), and 24 weeks (n = 6). Values for 2 weeks are significantly less ($P < .05$) than for 4 weeks, 16 weeks, and 24 weeks. Ten-week values are significantly less ($P < .05$) than 24-week values.

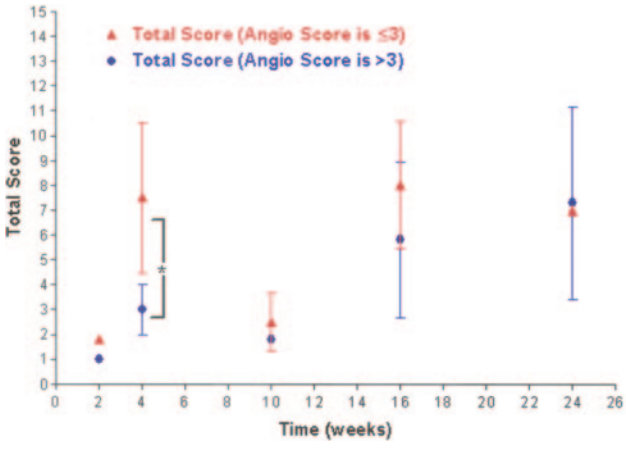

Fig 5. A comparison of healing (total score) over time between broad-necked (closed blue circle; >3) and small-necked (closed red triangle; ≤3) aneurysms. Data are represented by mean ± SD. There was a significant difference between the 2 groups (indicated by an asterisk) at the 4-week time period.

mon, so recanalization could not be applied to this model. Previous authors, however, have demonstrated in experimental aneurysms in rabbits that, even without evident recanalization on an angiogram, substantial coil compaction/recanalization may be seen histologically.[18] Thus, histologic criteria were applied for recanalization in this model.

Other investigators, specifically those using the swine model, have focused on extent of neck coverage seen on gross examination as a primary measure of healing.[15,16] It is difficult to calculate precise degrees of neck coverage across rabbit aneurysms when mean neck dimensions are 3–4 mm. Instead, this metric is incorporated as one of many in the assessment tool. Finally, tissue thickness over the coils along the neck has been proposed as a quantifiable outcome in other models. However, in light of the complex nature of the coil/parent artery interface, it is difficult, if not impossible, to determine a meaningful measure of tissue thickness. Such a measurement would depend on the exact location of the histologic section with respect to the coil mass and the aneurysm wall. Thus, a specific measurement of neck thickness was not incorporated into the scale.

There are several shortcomings in the proposed scale. First, the scale is based on these investigators' biases of idealized healing. Further work is required to validate the proposed scale. Additional study on the impact of aneurysm neck size on healing will need to be examined further, with larger numbers of subjects over time. It remains to be seen whether these results can be generalized to other institutions. Improved understanding of the effects of aneurysm size and packing attenuation would be needed to appropriately power future studies of endovascular devices with this model. Finally, correlation with human histologic findings after successful and failed endovascular occlusion will eventually be required to validate any animal model.

Conclusions

This proposed ordinal outcome scale can be applied to study of results following coil embolization of experimental aneurysms. The scale offers an appropriate dynamic range. The scale is also capable of detecting statistically significant differences in healing across time and between narrow- and wide-necked aneurysms.

Acknowledgments

Figs 1*A* and 2*A* used in this report also appeared as part of the article "Modified histologic technique for processing metallic coil-bearing tissue" (Dai D, Ding YH, Danielson MA, et al. *AJNR Am J Neuroradiol* 2005;27:1932–36) describing our modified histologic technique for processing metallic coil-bearing tissue.

References

1. Guglielmi G, Ji C, Massoud T, et al. **Experimental saccular aneurysms. II. A new model in swine.** *Neuroradiology.* 1994;36:547–50
2. Graves V, Partington C, Rufenacht D, et al. **Treatment of carotid artery aneurysms with platinum coils: an experimental study in dogs.** *AJNR Am J Neuroradiol* 1990;11:249–52
3. Graves V, Strother C, Rappe A. **Treatment of experimental canine carotid aneurysms with platinum coils.** *AJNR Am J Neuroradiol* 1993;14:787–93
4. Mawad M, Mawad J, Cartwright JJ, et al. **Long-term histopathologic changes in canine aneurysms embolized with Guglielmi detachable coils.** *AJNR Am J Neuroradiol* 1995;16:7–13
5. Reul J, Weis J, Spetzger U, et al. **Long-term angiographic and histopathologic findings in experimental aneurysms of the carotid bifurcation embolized with platinum and tungsten coils.** *AJNR Am J Neuroradiol* 1997;18:35–42
6. Bocher-Schwarz H, Ringel K, Bohl J, et al. **Histological findings in coil-packed experimental aneurysms 3 months after embolization.** *Neurosurgery* 2002;50:379–84
7. Tenjin H, Fushiki S, Nakahara Y, et al. **Effect of Guglielmi detachable coils on experimental carotid artery aneurysms in primates.** *Stroke* 1995;26:2075–80
8. Kallmes D, Helm G, Hudson S, et al. **Histologic evaluation of platinum coil embolization in an aneurysm model in rabbits.** *Radiology* 1999;213:217–22
9. Altes TA, Cloft HJ, Short JG, et al. **Creation of saccular aneurysms in the rabbit: a model suitable for testing endovascular devices.** *AJR Am J Roentgenol* 2000;174:349–54
10. Fujiwara N, Cloft H, Marx W, et al. **Serial angiography in an elastase-induced aneurysm model in rabbits: evidence for progressive aneurysm enlargement after creation.** *AJNR Am J Neuroradiol* 2001;22:698–703
11. de Gast A, Altes T, Marx W, et al. **Transforming growth factor beta-coated platinum coils for endovascular treatment of aneurysms: an animal study.** *Neurosurgery* 2001;49:690–94
12. Marx W, Cloft H, Helm G, et al. **Endovascular treatment of experimental aneurysms by use of biologically modified embolic devices: coil-mediated intraaneurysmal delivery of fibroblast tissue allografts.** *AJNR Am J Neuroradiol* 2001;22:323–33
13. Kallmes D, Fujiwara N, Yuen D, et al. **A collagen-based coil for embolization of saccular aneurysms in a New Zealand white rabbit model.** *AJNR Am J Neuroradiol* 2003;24:591–96
14. Kallmes D, Fujiwara N. **New expandable Hydrogel-platinum coil hybrid device for aneurysm embolization.** *AJNR Am J Neuroradiol* 2002;23:1580–88
15. Murayama Y, Vinuela F, Tateshima S, et al. **Bioabsorbable polymeric material coils for embolization of intracranial aneurysms: a preliminary experimental study.** *J Neurosurg* 2001;94:454–63
16. Murayama Y, Tateshima S, Gonzalez N, et al. **Matrix and bioabsorbable polymeric coils accelerate healing of intracranial aneurysms: long-term experimental study.** *Stroke* 2003;34:2031–37
17. Raymond J, Salazkin I, Georganos S, et al. **Endovascular treatment of experimental wide neck aneurysms: comparison of results using coils or cyanoacrylate with the assistance of an aneurysm neck bridge device.** *AJNR Am J Neuroradiol* 2002;23:1710–16
18. Fujiwara N, Kallmes D. **Healing response in elastase-induced rabbit aneurysms after embolization with a new platinum coil system.** *AJNR Am J Neuroradiol* 2002;23:1137–44